CATION-INDUCED ATTACHMENT OF CILIARY DYNEIN CROSS-BRIDGES

FRED D. WARNER. From the Department of Biology, Biological Research Laboratories, Syracuse University, Syracuse, New York 13210

ABSTRACT

Isolated, demembranated *Unio* gill cilia that have been activated and fixed for thin-section electron microscopy in the presence of 2 mM $MgSO_4$ have 87% of their outer dynein arms attached to an adjacent B subfiber. The distribution of attached arms is uniform with respect to doublet position in the cilium. When both 0.1 mM ATP and Mg^{++} are added to the activation and fixation solutions, the frequency of bridged arms is reduced to 48%. At the same time, the distribution of the attached arms appears to have been systematically modified with respect to doublet position and the active bend plane. Those doublet pairs positioned in the bend plane where interdoublet sliding is minimal retain a greater number of bridged arms than those doublet pairs positioned outside the bend plane where sliding is maximal. These observations imply a functional coupling of the Mg^{++}-induced bridging of the dynein arms and the subsequent binding and hydrolysis of ATP that results in a force-generating cross-bridge cycle.

KEY WORDS motility · cilia · microtubules dynein · cross-bridges · Mg^{++} · ATP

The ATPase or dynein arms of cilia and flagella generate the force required for microtubule sliding in an ATP-Mg^{++}-dependent cross-bridging interaction between the terminal subunit of the arms and protofilaments in the B subfiber. The cross-bridging phenomenon is analogous to the myosin-actin interactions of skeletal muscle but apparently only in the way that mechanical and energy-dependent aspects of sliding filament mechanisms must necessarily be equivalent. It has become increasingly apparent that the protein chemistry and molecular behavior of the two systems are unique processes, presumably having evolved independently but nevertheless possessing similar mechanochemical properties.

Although we were recently able to characterize the structural organization of ciliary dynein (11, 12), the molecular conditions under which dynein will both associate with and dissociate from B-subfiber tubulin are uncertain. After permitting isolated *Tetrahymena* cilia to slide apart actively in the presence of ATP-Mg^{++}, we (11) demonstrated an apparently stable dynein arm cross-bridge in axonemes that had been negatively contrasted for electron microscopy. In the presence of the nucleotide-cation complex, the arms were found to be attached to an adjacent B subfiber, whereas in their absence the arms were relaxed. In both the bridged and relaxed states, the arms had the same 32° base-directed polarity. These observations led us to suggest that the bridged arms represented the first step of a force-generating cross-bridge cycle and that preservation of the bridges was related in some way to the presence of ATP-Mg^{++}, and thus was motility dependent (11).

We now find, however, the latter part of this interpretation to have been in error.

In the present study, isolated lamellibranch gill cilia were fixed for thin-section electron microscopy in the individual presence of Mg^{++}, ATP,

and ATP-Mg^{++}. Mg^{++} causes all dynein arms in an axoneme profile to become attached to an adjacent B subfiber. The addition of ATP modifies the distribution of the dynein bridges so that it then corresponds to predicted values for sliding between each pair of doublet microtubules. The fixation procedure also reveals several related morphological alterations to the axoneme structure.

MATERIALS AND METHODS

Gill cilia from the fresh water lamellibranch mollusc *Unio* were isolated, demembranated, and purified according to procedures previously reported (12). Isolated cilia were routinely suspended in a minimal solution consisting of 40 mM *N*-2-hydroxymethylpiperazine-*N'*-2-ethane sulfonic acid (HEPES) and 0.1 mM dithiothreitol (DTT) at pH 7.4. Cilia were then activated by the addition of 0.1 mM ATP and 2 mM $MgSO_4$. Although these conditions were rarely adequate for uniform resumption of ciliary beating, they were nonetheless used in order to overcome variables otherwise introduced by the addition of other components to the activation solution.

However, the composition of the minimal solution is sufficient to consistently activate the sliding mechanism in these cilia. Samples of isolated cilia were routinely treated with trypsin (500:1 ratio) which permits their active sliding disintegration when subsequently activated by ATP-Mg^{++} (9). By using this simple test, it was found that the sliding mechanism was functional in every preparation of cilia studied.

Fixation for Electron Microscopy

Isolated, demembranated cilia were fixed for thin-section microscopy under four conditions with respect to the composition of the activation and fixation solutions: (*a*) 40 mM HEPES, 0.1 mM DTT, pH 7.4; (*b*) 40 mM HEPES, 0.1 mM DTT, 2 mM $MgSO_4$, pH 7.4; (*c*) 40 mM HEPES, 0.1 mM DTT, 2 mM $MgSO_4$, 0.1 mM ATP, pH 7.4; and (*d*) 40 mM HEPES, 0.1 mM DTT, 0.1 mM ATP, pH 7.4.

The four activation and four fixation solutions differ only with respect to the addition of 4% ultrapure glutaraldehyde to the fixation solutions.

Cilia were fixed by adding equal volumes (1–2 ml) of cilia suspended in each of the four activation solutions to each of the four respective fixation solutions (2% final glutaraldehyde concentration). These suspensions (4°C) were immediately centrifuged for 30–45 min at 50,000 *g*. The pellets thus obtained were rinsed for 1–2 min in their activation solutions and postfixed for 30–60 min in 1% OsO_4 containing the activation ingredients. The fixed pellets were dehydrated in ethanol series and embedded in Epon 812.

Silver interference-color sections were stained with 4% aqueous uranyl acetate for 15 min followed by staining in Reynolds' lead citrate for 2–5 min. Electron micrographs were calibrated by the use of available internal standards and carbon grating replicas.

RESULTS

All data are obtained from transverse sections of isolated *Unio* gill cilia. Individual doublet microtubules are numbered according to their position relative to doublets 5 and 6, recognized by the constantly bridged dynein arms occurring between these two doublets (10). In the figures, doublets 5–6 are located in the 6 o'clock position, and ascending doublet numbers then proceed in a clockwise (arm) direction when the axoneme is viewed from base-to-tip orientation (Fig. 1). The plane between doublets 1 and 5–6 (vertical axis) is the plane of active bending, and it occurs at a right angle to the plane of the central pair microtubules (horizontal axis). The precise positioning of doublets 1 and 5–6 relative to the central pair tubules permits unequivocal identification of these doublets even when all doublets are bridged by their dynein arms.

In order to simplify the treatment of numerical data pertaining to dynein cross-bridge frequency and distribution, the doublet 5–6 bridged arms are counted like those arms occurring between any other pair of doublets, even though the doublet 5–6 bridge frequency is greater than 97% under all conditions studied.

For purposes of scoring the dynein arms as being either bridged or unbridged, two criteria were used. First, the arms must appear to be structurally attached to an adjacent B subfiber, and second, the doublets thus joined must show a measurable spacing decrease of 10–16%. Furthermore, although both the inner and outer rows of arms appear to be equally affected by the experimental procedures, only the outer rows of arms were scored in order to eliminate possible ambiguities caused by the traditional lack of structural definition associated with the inner rows of arms.

Dynein Arms in the Relaxed Condition

Isolated cilia activated in 40 mM HEPES and 0.1 mM DTT alone or containing 0.1 mM ATP, and subsequently fixed in the same solutions, have the characteristic morphology and dimensions traditionally associated with cilia and flagella (Fig. 1, Table I, and reference 10). With the single exception of the doublet 5 arms, neither the inner nor

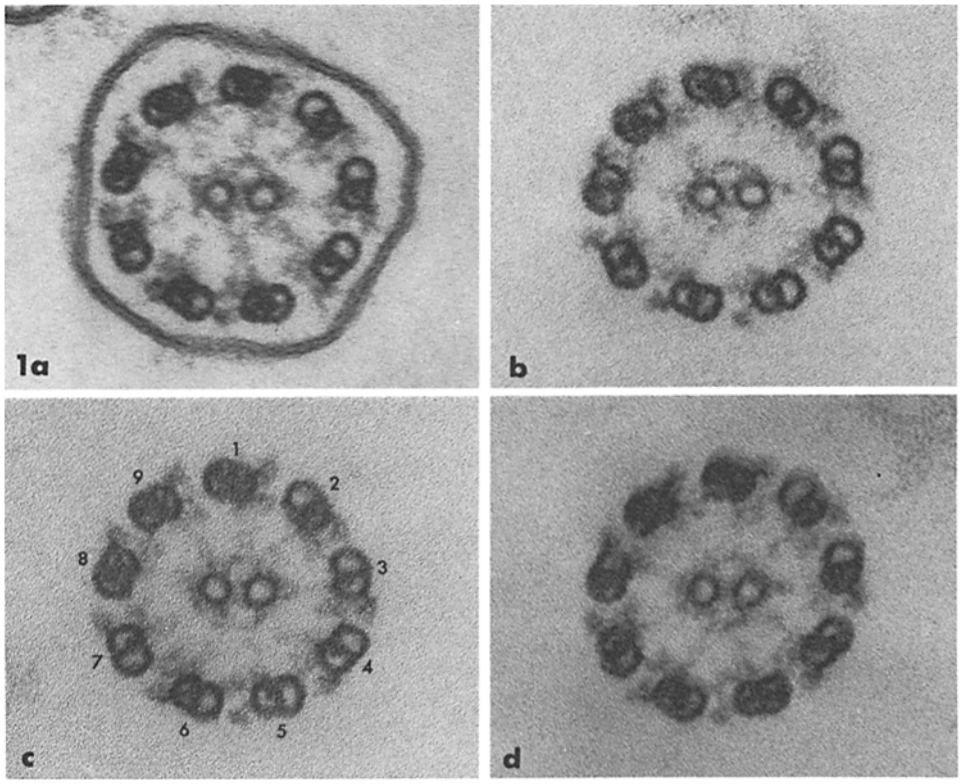

FIGURE 1 Control cilia, transversely sectioned and oriented so that doublets 5–6 are in the 6 o'clock position. (*a*) Intact, and (*b* and *c*) isolated cilia fixed in 40 mM HEPES-0.1 mM DTT-2% glutaraldehyde. (*d*) Isolated cilium fixed in the added presence of 0.1 mM ATP. All cilia appear to have normal morphology and dimensions. × 176,000.

outer rows of dynein arms appear in close proximity to adjacent B subfibers. A relatively constant 190-Å interdoublet spacing and 2,000-Å axoneme diameter are maintained in these cilia. The only unique structural properties of gill cilia are the aforementioned doublet 5–6 bridge and a slight compression of the axoneme profile in the bend plane (7). This compression results in a mean horizontal to vertical axis diameter ratio of 1.04. The compression occurs in both native and isolated cilia (Fig. 1) and is not related to the plane of sectioning.

Dynein Arms in the Presence of Mg^{++}

Isolated cilia, activated and fixed in the presence of 2 mM $MgSO_4$, have a strikingly different appearance with respect to both morphology and dimensions (Fig. 2 and Table I). The mean diameter of the axoneme has decreased to 1,680-Å (14.2% decrease), along with a corresponding 14% decrease in the interdoublet spacing. At the same time, the bend plane compression of the axoneme has increased to a ratio value of 1.23, indicating that the visibly obvious compression is not simply an illusion caused by the decrease in diameter.

Most importantly, however, the dynein arms of Mg^{++}-fixed cilia appear to be uniformly attached to their adjacent B subfibers (Fig. 2). Three separate preparations of cilia were examined, and in each (200 count) more than 95% of the axonemes visible in clear profile had two or more pairs of doublets bridged by their dynein arms. The frequency distribution of the bridged arms relative to the numbered doublet pairs is shown in Table II and Fig. 3. The mean frequency of bridging for all doublets is 87.3 ± 6%, which corresponds to an average number of 7.9 bridged doublets (nine possible) per axoneme cross section. The distribution of bridged arms appears to be generally uniform with respect to doublet number (position), although doublet pairs 1–2, 2–3,

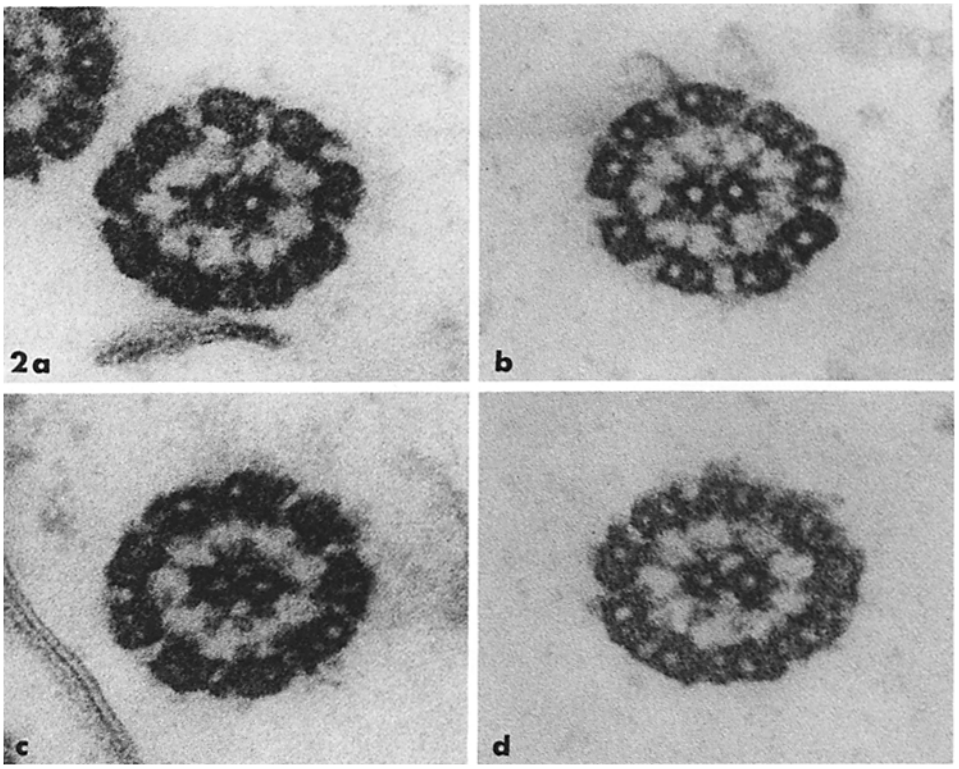

FIGURE 2 Isolated cilia activated and fixed in the presence of 2 mM $MgSO_4$. The cilia show a 14% decrease in diameter as well as compression in the bend plane (vertical axis). Most of the dynein arms appear to be attached to their neighboring B subfibers, reflecting an overall bridging efficiency of 87% (see Fig. 3). × 176,000.

3–4, and 7–8 may have slightly fewer bridged arms than doublet pairs 4–5, 5–6, 6–7, and 8–9 (see below).

Although, by definition, arm attachment to a B subfiber is based on two structural criteria, the following observations support the interpretation that the arms are functionally attached to the B subfiber. (*a*) Arm cross-bridging is supported by cations that support sliding (Mg^{++}, Ca^{++}, and reference 9). (*b*) Cilia activated and fixed in the presence of either 2 mM or 200 mM KCl retain normal morphology and dimensions. (*c*) Arm cross-bridging is systematically modified by the addition of hydrolyzable substrate (see below). (*d*) Cilia whose arms have been partially extracted by KCl (12) before fixation in the presence of Mg^{++} show both a disruption to the axoneme profile and an increased doublet spacing (>190 Å) in regions where the arms are absent. (*e*) Arm cross-bridging is maintained in Mg^{++}-fixed cilia that have broken open and lost their radial spoke attachments to the central pair tubules.

Dynein Arms in the Presence of ATP-Mg^{++}

Isolated cilia activated and fixed in the combined presence of 0.1 mM ATP and 2 mM $MgSO_4$ have a similar general appearance (Fig. 4) and dimensions as Mg^{++}-fixed cilia, although there has been a small increase in axoneme diameter and a corresponding decrease in the compression ratio (Table I). Three separate preparations were examined (200 count each) and more than 91% of the axonemes retained two or more pairs of doublets bridged by their dynein arms. However, the mean frequency of bridging for all doublets is reduced to 48.3% or 4.3 bridges per axoneme cross section (Table I). The frequency distribution of bridged doublets in these cilia is shown in Fig. 5 and Table II. Not only has a substantial decrease occurred in the number of bridged doublets, the decrease is clearly systematic with respect to doublet number (position) in the axoneme. Doublet pairs 9–1, 1–2, 4–5, 5–6, and 6–7 (bend plane, vertical axis; see Fig. 1) retain a greater number of

TABLE I

Functional Characteristics of Transversely Sectioned Unio Cilia

Fixation conditions	Motility	Cilium diameter*	Axis ratio‡	Doublet spacing§	Bridge frequency‖
		Å		Å	%
Intact cilium (HEPES)	–	2,000	1.04	190 (163)	11
Isolated cilium (HEPES)	–	2,000	1.04	190 (163)	11
Isolated cilium (HEPES-ATP)	–	2,000	1.04	190 (163)	11
Isolated cilium (HEPES-Mg^{++})	–	1,680	1.23	163	87
Isolated cilium (HEPES-ATP-Mg^{++})	+	1,750	1.10	163-190	48

* Mean value of the doublets 1-5 and 3-8 axes, measured at the centrifugal surface of subfiber B.

‡ Diameter at doublets 3-8/doublets 1-5.

§ Number in parentheses is the doublets 5-6 bridge. Measured at the closest apposed doublet surfaces.

‖ Percent of total outer dynein arm sites occurring in the bridged condition. The 11% value is for the doublets 5-6 bridge.

TABLE II

*Frequency Distribution of Bridged Dynein Arms**

Conditions	Doublet pairs								
	1-2	2-3	3-4	4-5	5-6	6-7	7-8	8-9	9-1
	% bridged arms								
HEPES	<0.1	<0.1	<0.1	<0.1	98	<0.1	<0.1	<0.1	<0.1
HEPES-ATP	<0.1	<0.1	<0.1	<0.1	97	<0.1	<0.1	<0.1	<0.1
HEPES-Mg^{++}	82	79	94	91	98	88	83	93	88
HEPES-Mg^{++}-ATP	62	38	33	48	98	55	22	32	55

* 120 Axonemes were counted for each of the four conditions. Percent bridged arms is the number of outer arms structurally attached to an adjacent B subfiber as determined for each pair of doublets in the axoneme. Thus a maximum of 120 bridged arms (100%) were possible for each doublet site. The data for Mg^{++} and Mg^{++}-ATP conditions are plotted in Figs. 3 and 5.

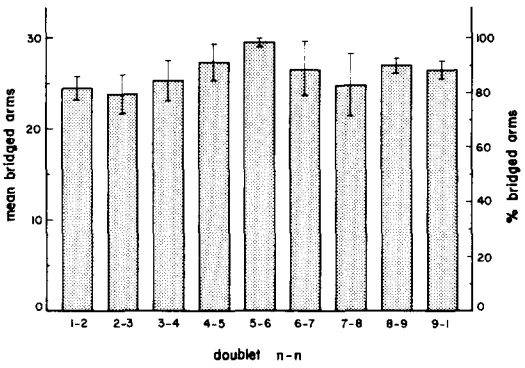

FIGURE 3 Distribution profile of bridged dynein arms for cilia fixed in the presence of 2 mM $MgSO_4$. The mean number of bridged arms per doublet pair (n-n) was determined from four groups of 30 cilia each (120 total possible bridges per doublet pair). The vertical bars represent the SD associated with the four groups. The percent bridged arms is the mean bridging frequency for each doublet pair which converts to a frequency of 87% for all doublets.

bridged arms (64%) than doublet pairs 2-3, 3-4, 7-8, and 8-9 (31%) (horizontal axis). This distribution appears to be related to the plane of active bending and interdoublet sliding (see Discussion). However, doublets on the left side of the axoneme (5-6-7-8-9-1) retain about the same number of bridged arms (52%) as doublets on the right side (1-2-3-4-5-6) (56%), and doublets at the top of the axoneme (8-9-1-2-3) retain about the same number of bridged arms (47%) as doublets at the bottom (3-4-5-6-7-8) (51%).

Although the bridge distribution is based on relatively few counted cilia (four groups of 30 cilia each), the distribution profile is established and maintained after counts of only 5-10 cilia. The aforementioned observations concerning the functional nature of Mg^{++}-induced arm attachment to the B subfiber are applicable to ATP-Mg^{++}-activated cilia as well.

DISCUSSION

The recent description of dynein cross-bridges in ATP-Mg^{++}-disintegrated *Tetrahymena* cilia (11) suggested that arm attachment to the B subfiber was supported by the nucleotide-cation complex. In the present study, it was reasoned that, by maintaining millimolar quantities of nucleotide and cation in the activation and fixation solutions, it should be possible to support dynein bridging long enough for the fixative's protein cross-linking properties to join permanently the attached arms to the B subfiber and thus make them visible for thin-section electron microscopy.

Indeed, the method appears to work; however, the results of the present study clearly indicate

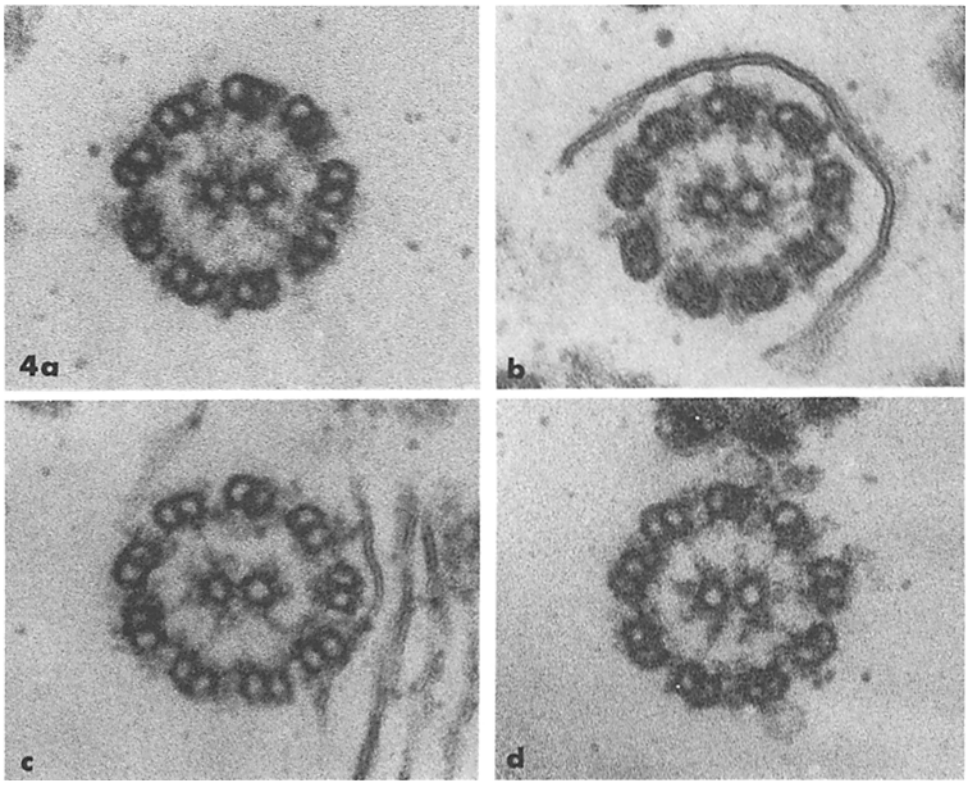

FIGURE 4 Isolated cilia activated and fixed in the presence of 2 mM $MgSO_4$ and 0.1 mM ATP. The cilia have dimensions and morphology similar to those of the Mg^{++}-fixed cilia; however, the bridging frequency for all doublets is reduced to 48%, and the bridge distribution has been systematically modified (see Fig. 5). × 176,000.

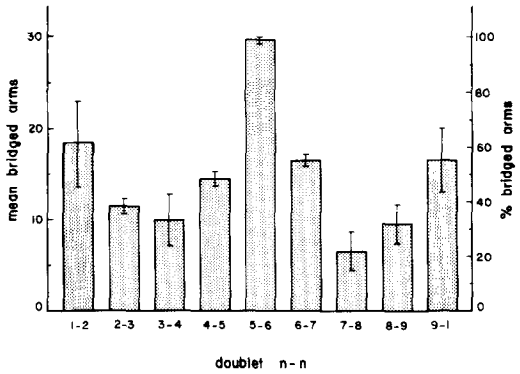

FIGURE 5 Distribution profile of bridged dynein arms for cilia fixed in the presence of 2 mM $MgSO_4$ and 0.1 mM ATP. The mean number of bridged arms per doublet pair (n-n) was determined from four groups of 30 cilia each (120 total possible bridges per doublet pair). The vertical bars represent the SD associated with the four groups. The distribution profile is clearly systematic with respect to the vertical (doublets 9-1-2 and 5-6) and horizontal (doublets 3-4 and 7-8) axes of the cilium. The percent bridged arms is the mean bridging frequency for each doublet pair which converts to a frequency of 48% for all doublets.

that attachment of the dynein arms to the B subfiber is dependent only on the presence of an appropriate divalent cation (Mg^{++}). Bridged dynein arms are not preserved in cation-free fixatives, presumably because the native cation concentration in the organelle falls below a threshold value that will support bridging. Although detailed interpretation of the results must await the outcome of in-progress experiments designed to determine the conditions under which isolated dynein will functionally associate with the B subfiber, some preliminary comments on the nature of the dynein cross-bridging mechanism can be made.

Mg^{++}-induced dynein bridges occur in more than 96% of the cilia counted. Within these cilia. 7.9 cross-bridges occur per cilium cross section

(Tables I and II). This represents an Mg^{++}-related bridging efficiency of 87% and suggests that attachment of the arms to the B subfiber occurs simultaneously and uniformly along the length of the cilium.

When both Mg^{++} and ATP are added to cilia, the bridged arm frequency is reduced to 48% (4.3 bridges per axoneme) and the bridges show an altogether different distribution profile (Fig. 5). The retention (or release) of bridged arms appears to be related to the active bend plane of the cilium. Those doublet pairs positioned at right angles to the bend plane retain a greater number of bridged arms than those doublet pairs positioned parallel to the bend plane. When the bridge distribution is compared with predicted values of interdoublet sliding for lamellibranch cilia (Table III in reference 10), an inverse relationship between the number of bridged arms and the amount of doublet sliding becomes apparent. For example, doublets 3–4 and 7–8 exhibit maximal predicted sliding during a bend, and yet these doublets retain the lowest frequency of bridged arms. Similarly, doublets 9–1–2 and 5–6, in the bend plane, show minimal predicted sliding, but they retain the greater frequency of bridged arms.

Although the fit of bridged arms to interdoublet sliding is not exact, it is close enough to be more than a circumstantial occurrence, particularly when taking into consideration that the bend-twist condition of the ATP-Mg^{++}-fixed cilia is not known. The distribution data are consistent with the observation of Satir and Sale (8) that active sliding appears to be centered around doublets 3 and 8 in ATP-Mg^{++}-disintegrated *Tetrahymena* cilia. Furthermore, the data imply functional coupling of the Mg^{++}-induced bridges with an ATP hydrolysis cycle and are consistent with our earlier suggestion (11) that active sliding is basically a two-part phenomenon. The first sequence of activities would involve the Mg^{++}-related attachment of the dynein cross-bridge while the second sequence of events would involve the binding and hydrolysis of ATP by the cross-bridge, resulting in the generation of force and release of the cross-bridge. The latter sequence would also require regulatory activity to specify those doublets, e.g., 3–4 or 7–8, which are to slide actively or passively (effective or recovery strokes). In other words, the bridged arms would inhibit sliding between all doublets until the arms along those doublets important in an effective or recovery stroke were either activated or relaxed. The distribution data imply that such behavior is an intrinsic part of the structure chemistry of the cilium, and since isolated cilia can be induced to beat quite normally, that behavior must be independent of any cell surface phenomena that may otherwise exert influence on the ciliary beat (5).

If it is assumed that the bridged arms retained in both Mg^{++} and ATP-Mg^{++} are in identical conformational-functional states with respect to a potential cross-bridge cycle, then the addition of ATP must either cause the systematic relaxation of bridges between specific doublets or preferentially activate those bridges to complete their cross-bridge cycles and detach. In the latter instance, reattachment of the arms (motility) would eventually be blocked by the effects of the added glutaraldehyde fixative. If this interpretation is correct, the distribution of the bridges in ATP-Mg^{++} can be expected to mimic the bridge distribution in motile cilia. If the observed bridge distribution were not coupled to motion, one would expect that the addition of ATP would cause the wholesale dissociation of the bridges, similar to the way in which ATP dissociates myosin HMM from F-actin (4). Similar reasoning, plus the 20:1 ratio of Mg^{++} to ATP, suggests that arm detachment does not result from simple chelation of Mg^{++} by the nucleotide.

At present, the polarity and functional state of the dynein bridges in *Unio* cilia can only be assumed to be the equivalent of the ATP-Mg^{++} bridges described in *Tetrahymena* cilia (6, 11). It may be noted, however, that D. R. Mitchell (unpublished results) has preserved bridged dynein arms in *Tetrahymena* cilia by using methods identical to those reported here. We previously noted (11) that, because of the orientation of the ATP-Mg^{++}-related bridges, in terms of a potential cross-bridge cycle the dynein bridges could not be in the same physiological state as myosin rigor cross-bridges, and therefore the cross-bridging cycles of the two systems appear to exhibit important differences in regard to the preservation of stable cross-bridges.

The apparent conflict between the observed ATP-Mg^{++}-related dynein cross-bridges in *Tetrahymena* (and now *Unio*) cilia (11) and the retention of a rigorlike bend form and dynein cross-bridges in sea urchin sperm flagella (2, 3) may be resolved by the present observations. In order to induce the rigorlike condition, the bend forms of actively beating sperm flagella (3) were arrested by dilution of available ATP to nonphysiological

levels. However, dilution was done with buffer containing 2 mM $MgSO_4$. The present observations suggest that the stable Mg^{++} concentration would support continued arm bridging and maintain the arrested bend form of the organelle independent of the absence of ATP. The subsequent addition of small quantities of ATP (insufficient to cause resumption of beating) was found to relax the flagella, presumably by activating rather than relaxing the attached arms. Strictly speaking, then, it may not have been the absence of ATP that preserved attachment of the dynein arms and thus retention of the rigorlike bend form, but rather it may have been the presence of Mg^{++} that maintained a stable arm attachment and thus preserved the bend form. The rigorlike sperm flagella were also fixed for electron microscopy (2), and bridged arms similar to those described here were seen. However, it was noted that preservation of the bend and cross-bridges was highly sensitive to the method of fixation, as would be expected if dynein-associated Mg^{++} were diffusing into a Mg^{++}-free fixative, resulting in gradual relaxation of the bridged arms.

Bloodgood (1) has described properties of cross-bridges between microtubules in the axostyle of *Saccinobaculus* similar to those found in *Unio* and *Tetrahymena* cilia. On the basis of studies of relaxed and coiled (ATP-Mg^{++}) states of the axostyle, he concluded that stable cross-bridges were supported by the nucleotide-cation complex. He also observed that the coiled state was relaxed by the addition of EDTA (a Mg^{++} chelator) and therefore suggested that the cross-bridges had separate cation- and nucleotide-cation-binding sites. Although it has not yet been determined where nucleotide-free Mg^{++} is binding in order to permit ciliary dynein bridging, the present data clearly indicate a specific role for divalent cation that is independent of substrate-cation interactions. Furthermore, the cation-binding site must be relatively nonspecific since Mg^{++}, Ca^{++}, and Mn^{++} all support motility (sliding) (9) and thus, it must be assumed, the formation of cross-bridges.

In conclusion, while several aspects of these interpretations are preliminary, with the publication of this and several recent studies (6, 9, 11, 12) it is apparent that a solid conceptual basis now exists on which to formulate experimental studies on the dynein cross-bridge mechanism.

This study was supported by research grant GM20690 from the National Institutes of Health.

Received for publication 10 February 1978, and in revised form 15 March 1978.

REFERENCES

1. Bloodgood, R. A. 1975. Biochemical analysis of axostyle motility. Cytobios. **14**:101-120.
2. Gibbons, I. R. 1975. The molecular basis of flagellar motility in sea urchin spermatozoa. *In:* Molecules and Cell Movement. S. Inoué and R. E. Stephens, editors. Raven Press, New York. 207-231 pp.
3. Gibbons, B. H., and I. R. Gibbons. 1974. Properties of flagellar "rigor waves" formed by abrupt removal of adenosine triphosphate from actively swimming sea urchin sperm. *J. Cell Biol.* **63**:970-985.
4. Huxley, H. E. 1963. Electron microscope studies on the structure of natural and synthetic protein filaments from striated muscle. *J. Mol. Biol.* **7**:281-308.
5. Kung, C. 1976. Membrane control of ciliary motions and its genetic modification. *In:* Cell Motility. Vol. C. R. D. Goldman, T. D. Pollard and J. L. Rosenbaum, editors. Cold Spring Harbor Laboratory Press, Cold Spring Harbor, New York. 941-948 pp.
6. Sale, W. S., and P. Satir. 1977. Direction of active sliding in *Tetrahymena* cilia. *Proc. Natl. Acad. Sci. U. S. A.* **74**:2045-2049.
7. Satir, P. 1976. Production and arrest of ciliary motility. *In* Contractile Systems in Nonmuscle Tissues. S. V. Perry, A. Margreth, and R. S. Adelstein, editors. American Elsevier Press, New York. 263-273 pp.
8. Satir, P., and W. S. Sale. 1977. Tails of *Tetrahymena*. *J. Protozool.* **24**:498-501.
9. Summers, K. E., and I. R. Gibbons. 1971. Adenosine triphosphate-induced sliding of tubules in trypsin-treated flagella of sea urchin sperm. *Proc. Natl. Acad. Sci. U. S. A.* **68**:3092-3096.
10. Warner, F. D. 1976. Cross-bridge mechanisms in ciliary motility: the sliding-bending conversion. *In:* Cell Motility. Vol. C. R. D. Goldman, T. D. Pollard, and J. L. Rosenbaum, editors. Cold Spring Harbor Laboratory Press, Cold Spring Harbor, New York. 891-914 pp.
11. Warner, F. D., and D. R. Mitchell. 1978. Structural conformation of ciliary dynein arms and the generation of sliding forces in *Tetrahymena* cilia. *J. Cell Biol.* **76**:261-277.
12. Warner, F. D., D. R. Mitchell, and C. R. Perkins. 1977. Structural conformation of the ciliary ATPase dynein. *J. Mol. Biol.* **114**:367-384.